International Journal of Computer Science & Mechatronics
A peer reviewed International Journal | Article Available online www.ijcsm.in
©smsamspublications.com | Vol.2.Issue 2.2016

Estimation and Correction of Offset Errors in LTE Systems

Research Article
ISSN: 2455-1910

Mr.K.Vijay[1], Mr.G.V.Ramanaiah[2]
Assistant Professor of ECE, Associate Professor of ECE at PSCMR College of Engineering & Technology

Abstract: In this paper, we show an information based technique for synchronous Maximum Likelihood (ML) image timing and bearer recurrence counterbalance estimation in Orthogonal recurrence division multiplexing (OFDM) frameworks. The cyclic augmentation, a gatekeeper space going before OFDM edges, is of unequivocal significance for this strategy. It is demonstrated that the repetition presented by this cyclic augmentation permits the estimation to be performed without extra pilots. Reproductions demonstrate that the execution of the recurrence estimator is usable in a following mode while the planning estimation can be utilized as a part of a securing mode. A concurrent estimator of timing and recurrence counterbalance in OFDM frameworks, which needn't bother with pilots yet utilizes the repetition presented by the cyclic expansion, has been displayed. It is determined under the presumption that the channel just comprises of added substance clamor. Reproductions demonstrate that in a dispersive blurring environment the planning estimator can be utilized as a part of an obtaining mode and the recurrence estimator may perform well in a following mode. In a remote framework, pilots are required for channel estimation. These known images can be utilized by the estimator and consequently assist expand the execution. Coming about synchronizers might be half breed structures utilizing both pilots and cyclic prefix. Step by step instructions to fuse pilot images in such planning and recurrence estimators are not clear and needs promote research.

Key Terms:

I.INTRODUCTION: To guarantee the most productive information transmission conceivable, there ought to be no requirements on the amount of the cyclic prefix (CP) is involved by intersymbol impedance (ISI). Here an answer for timing synchronization is proposed, that is, powerful notwithstanding when the most grounded multipath parts are deferred in respect to the main arriving ways. In this circumstance, existing strategies perform ineffectively, though the arrangement proposed utilizes the subsidiary of the relationship work and is less delicate to the channel drive reaction. In this paper, synchronization of a DVB single-recurrence system is examined. The procedure has significance to telecast, OFDMA, and WLAN applications, and reenactments are exhibited which contrast the strategy and existing methodologies. Another multipath-hearty OFDM timing estimation method in view of the subsidiary of the summed connection capacity has been proposed and the execution analyzed for the DVB-T framework. Indeed, even in the most pessimistic scenario considered of short CPs, the strategy has appeared to be better than the crest identification technique. In considering unpredictability, the synchronization calculations are ruled by the connection estimation, and the extra number of augmentations of the subordinate and LS fitting are

under 1%. An underlying limitation was that the ISI is constrained to the gatekeeper interim, however with the extra principles based preparing, this need not be the situation. Contrasted with the Beek and second subsidiary strategies, the primary subordinate technique offers reliably great assessments over an extensive variety of channels. Appraisals are still great notwithstanding when vast bits of the CP are involved by ISI. It ought to be noticed that the mean planning evaluation is one-sided contrasted with the perfect planning point. OFDM (Orthogonal Frequency Division Multiplexing)provides the promising physical layer for 4G and 3GPP LTE Systems as far as effective utilization of transmission capacity and information rates. This paper highlights the execution of OFDM in Digital Video Broadcasting-Terrestrial (DVB-T). It primarily concentrates on the planning balance issue present in OFDM frameworks and its proposed arrangement utilizing Cyclic Prefix (CP) as a changed SC (Schmidl and COX) calculation. It highlights the planning synchronization and execution examination through piece mistake rate. Synchronization issues in OFDM are vital and can prompt data misfortune if not legitimately tended to. Reproductions were performed to actualize DVB-T framework and to think about various. The fundamental target of this paper was to concentrate on and research the requirement for timing synchronization mistakes in OFDM framework, the significant impacts of timing counterbalance blunders, execution of framework with reference to BER and afterward to analyze a portion of the synchronization calculations. The objective was accomplished by executing the OFDM framework utilizing DVB-T as a case with the impact and also revision of timing jitter. On the closing comments, it was watched that AWGN environment was primitive and adequate to concentrate on the point though Fading environment gives the great picture of down to earth situation. The future work will include the examination and reproduction of various probabilistic models in best in class advancements, for example, 5G LTE.

II.THE DESIGN: The most challenging aspect of designing a communication system is the estimation and correction of synchronization errors that occur during transmission. Synchronization of the system in time and frequency is still the source of much research and yet is one of the most often overlooked subjects in published papers. This chapter is divided into two sections. The first gives mathematical descriptions of the synchronization errors present on OFDM systems. The effects of these errors on the received signals are analyzed and simulations of the errors are presented whose code can be found in Appendix D and Appendix E. The second section describes the estimation of the errors at the receiver. Figure 6.1 shows the block diagram of the synchronization process of a typical receiver. Simulations of the error estimations are presented using the IEEE802.11 standard for the OFDM frame structure

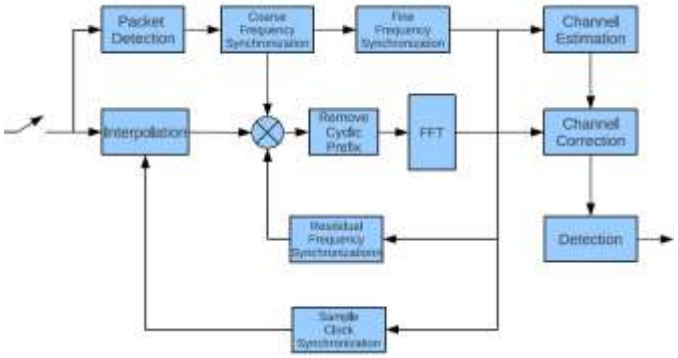

Figure: Synchronization blocks in OFDM receiver**.**

Synchronization Errors: In this section the effects of frequency and timing offsets will analyzed and simulated. As stated earlier, OFDM systems are very sensitive to frequency offsets between transmitter and receiver when modulating to pass band and back to baseband. Both ISI and inter channel interference (ICI) need to be mitigated as much as possible in order for the system to accurately receive data. Much of the ISI can be eliminated with the addition of a guard interval or cyclic prefix as discussed in chapter 4. ICI is affected by the orthogonality of the subcarriers, which can be caused by Doppler shift or the offset in carrier frequency between the transmitter and receiver. Not only must frequency offsets be dealt with but also the sample clock and the frame or FFT window timing. Offsets in timing can cause ISI as well as ICI. In this section we will consider carrier frequency offset, symbol timing, and frame start position. We will not consider Doppler shift, as our concern lies in systems that behave as stationary, i.e. IEEE 802.11.

Frequency Offset: Let Δf_c [Hz] be the carrier frequency offset and the normalized carrier frequency offset, ε , be

$$\varepsilon = \frac{\Delta f_c}{\Delta f}$$

Where Δf is the sub-carrier bandwidth (sub-carrier spacing). There is not only the possibility of carrier frequency offset between transmitter and receiver, but also a phase difference θ0. As before, let x[k] be the transmitted sample and h[k] the K^{th} tap of the multipath channel impulse response with NC taps. Then, the received nth estimated symbol is

$$\hat{X}[n] = \frac{1}{N}\sum_{k=0}^{N-1}\left(\sum_{l=0}^{N_c-1} h[l]\,x[k-l]\right) e^{-j2\pi\frac{nk}{N}} e^{j2\pi\frac{k\varepsilon}{N}} e^{j\theta_o}$$

Where $e^{-j2\pi\frac{nk}{N}}$ performs the demodulation via the FFT, $e^{j2\pi\frac{k\varepsilon}{N}}$ is the normalized carrier frequency, and $e^{j\theta_o}$ is the common phase rotation. Evaluating $\hat{X}[n]$ further we have

$$\begin{aligned}
\hat{X}[n] &= \frac{1}{N}\sum_{k=0}^{N-1}\sum_{l=0}^{N_c-1} h[l]\sum_{m=0}^{N-1} X[m] e^{-j\pi 2m\frac{k-l}{N}} e^{-j2\pi\frac{nk}{N}} e^{j2\pi\frac{k\varepsilon}{N}} e^{j\theta_o} \\
&= \frac{1}{N}\sum_{k=0}^{N-1} e^{j2\pi\frac{k\varepsilon}{N}} \sum_{l=0}^{N_c-1} h[l]\sum_{m=0}^{N-1} X[m] e^{-j\pi 2k\frac{n-m}{N}} e^{-j2\pi\frac{ml}{N}} e^{j\theta_o} \\
&= \frac{1}{N}\sum_{k=0}^{N-1} e^{j2\pi\frac{k\varepsilon}{N}} \sum_{m=0}^{N-1} X[m] e^{-j\pi 2k\frac{n-m}{N}} \sum_{l=0}^{N_c-1} h[l] e^{-j2\pi\frac{ml}{N}} e^{j\theta_o} \\
&= \frac{1}{N}\sum_{k=0}^{N-1} e^{j2\pi\frac{k\varepsilon}{N}} \sum_{m=0}^{N-1} X[m]H[m] e^{-j\pi 2k\frac{n-m}{N}} e^{j\theta_o} \\
&= \sum_{m=0}^{N-1} X[m]H[m]\frac{1}{N}\sum_{k=0}^{N-1} e^{j2\pi k\frac{(m-n+\varepsilon)}{N}} e^{j\theta_o}
\end{aligned}$$

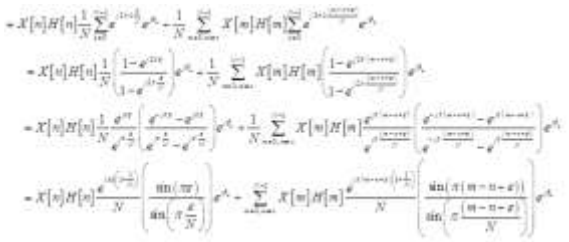

(6.3)

The first summand in equation 6.3 is the desired demodulated symbol on the nth sub-carrier with attenuation $\left(\frac{\sin(\pi\varepsilon)}{\sin\left(\pi\frac{\varepsilon}{N}\right)}\right)$ and phase rotations $\frac{e^{j\pi\varepsilon\left(1+\frac{1}{N}\right)}}{N}$ and $e^{j\theta_o}$. The second addend is the contribution of the remaining N − 1 sub-carriers with attenuation $\left(\frac{\sin(\pi(m-n+\varepsilon))}{\sin\left(\pi\frac{(m-n+\varepsilon)}{N}\right)}\right)$ and phase rotation $\frac{e^{j\pi(m-n+\varepsilon)\left(1+\frac{1}{N}\right)}}{N}$ and $e^{j\theta_o}$. This second summand results in ICI. The coefficients for the second summand are called the ICI coefficients and are described for the kth sub-carrier index as

$$ICI_N(k) = \frac{e^{j\pi(k+\varepsilon)\left(1+\frac{1}{N}\right)}}{N}\left(\frac{\sin(\pi(k+\varepsilon))}{\sin\left(\pi\frac{(k+\varepsilon)}{N}\right)}\right)$$

with ϱ = 0.5, 0.1, 0.05, 0.025.

$$\sum_{k=1}^{N-1}\left|ICI_N(k)\right|^2$$

Another helpful description is the carrier-to-interference p ower ratio [25] (CIR), which is analogous to SNR, is defined as

$$CIR = \frac{\left|ICI_N(0)\right|^2}{\sum_{k=1}^{N-1}\left|ICI_N(k)\right|^2}$$

Sampling Clock Offset: At the receiver the incoming signal is sampled with an analog to digital converter (ADC). The ADC is driven by the receiver clock which, in practice, is not perfectly synchronized with the transmitter clock. The derivation of the demodulated symbol with sampling period offset is similar to that of Section 6.1.1 where frequency offset was considered. To simplify the derivation, we assume an ideal channel with no other synchronization error present and no cyclic prefix. Let T and T′ be the transmitter and receiver sampling periods respectively and ϱ = T−T′ T be the sampling period offset. The continuous time transmitted signal is then

$$S_k(t) = \frac{1}{Nfft} \sum_{l=0}^{Nfft-1} X[l] e^{j2\pi l \frac{t}{NfftT}}$$

and the sampled signal at the output of the ADC with sampling period offset $\varepsilon = \frac{T' - T}{T}$ is

$$r[nT'] = s[nT']$$

$$= \frac{1}{Nfft} \sum_{l=0}^{Nfft} X[l] e^{j2\pi l \frac{nT'}{NfftT}}$$

$$= \frac{1}{Nfft} \sum_{l=0}^{Nfft} X[l] e^{j2\pi l \frac{n(1+\varepsilon)}{NfftT}}$$

The attenuation is dependent on sub-carrier index, sampling offset, and the number of sub-carriers. This would suggest that as the sub-carrier index increases, the attenuation decreases and the phase increases. Upon applying the baseband demodulation, the mth sub-carrier is

$$\bar{X}[m] = \sum_{n=0}^{2Nfft-1} S[nT'] e^{-j2\pi \frac{nm}{2Nfft}}$$

$$= \sum_{n=0}^{2Nfft-1} \left(\frac{1}{Nfft} \sum_{l=0}^{2Nfft} X[l] e^{j2\pi l \frac{n(1+\varepsilon)}{Nfft}} \right) e^{-j2\pi \frac{nm}{2Nfft}}$$

$$= \frac{1}{Nfft} \sum_{n=0}^{2Nfft-1} \sum_{l=0}^{2Nfft-1} X[l] e^{j2\pi l \frac{n}{2Nfft}} e^{j2\pi l \frac{n\varepsilon}{2Nfft}} e^{-j2\pi \frac{nm}{2Nfft}}$$

$$= \frac{1}{Nfft} \sum_{n=0}^{2Nfft-1} \sum_{l=0}^{2Nfft-1} X[l] e^{j2\pi n \frac{(l-m)}{2Nfft}} e^{j2\pi l \frac{n\varepsilon}{2Nfft}}$$

$$= \frac{1}{Nfft} \sum_{n=0}^{2Nfft-1} \sum_{l=0}^{2Nfft-1} X[l] e^{j2\pi n \frac{(l(1+\varepsilon)-m)}{Nfft}}$$

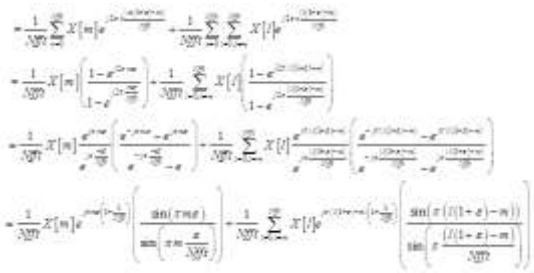

As with frequency offset, we have the desired demodulated sub-carrier X[m] with attenuation factor $\left(\frac{\sin(\pi m \varepsilon)}{\sin\left(\pi m \frac{\varepsilon}{Nfft}\right)} \right)$ and phase rotation $e^{j\pi m\varepsilon\left(1+\frac{1}{Nfft}\right)}$.By comparison, recall that the attenuation and phase for frequency offset is solely dependent on the frequency offset. Also present is ICI caused by the interaction of the remaining Nfft − 1 sub-carriers

$$ICI_\varepsilon[m] = \frac{1}{Nfft} \sum_{l=0, l\neq m}^{Nfft} X[l] e^{j\pi(l(1+\varepsilon)-m)\left(1+\frac{1}{Nfft}\right)} \left(\frac{\sin\left(\pi\left(l(1+\varepsilon)-m\right)\right)}{\sin\left(\pi \frac{\left(l(1+\varepsilon)-m\right)}{Nfft}\right)} \right)$$

where the ICI caused by the lth index is dependent on the desired sub-carrier index m and the sampling offset. To find the the power of the ICI, we assume that the X[k] are independently identically distributed (IID) so that

$$\begin{cases} E[X_k] = 0 \\ E[X_k X_r^*] = \delta_{k,r} \sigma_x^2 \end{cases}$$

where σ2x is the expected value of the power in the data symbols. The power of the ICI for the mth demodulated sub-carrier is then

$$E\left[ICI_\varepsilon(m) ICI_\varepsilon^*(m)\right] = \frac{1}{N_{fft}^2} \sum_{k=0, k\neq m}^{Nfft} E[X[k] X^*[k]] \left| \frac{\sin\left(\pi\left(k(1+\varepsilon)-m\right)\right)}{\sin\left(\pi \frac{\left(k(1+\varepsilon)-m\right)}{Nfft}\right)} \right|^2$$

$$= \frac{\sigma_x^2}{N_{fft}^2} \sum_{k=0, k\neq m}^{Nfft} \left| \frac{\sin\left(\pi\left(k(1+\varepsilon)-m\right)\right)}{\sin\left(\pi \frac{\left(k(1+\varepsilon)-m\right)}{Nfft}\right)} \right|^2$$

The signal to ICI power ratio is given by

$$SIR = \frac{\left|S_k(t)\right|}{E\left[ICI_\varepsilon(m) ICI_\varepsilon^*(m)\right]}$$

Frame Timing Offset: The estimation of the OFDM symbol or frame start position determines the alignment of the FFT window with the non-cyclically extended OFDM symbol. An offset in the FFT window can then include a neighboring OFDM symbol causing ISI, which can affect the orthogonality of the sub-carriers producing ICI. Analysis of the effects of frame timing offset on the constellation and the spectrum will be discussed with and without the use of a cyclic prefix for QPSK. We proceed first with the latter case.

Assuming no other synchronization errors and an ideal channel, the time series samples for the math OFDM symbol are

$$x_m[n] = \sqrt{\frac{1}{Nfft}} \sum_{k=0}^{Nfft-1} X_m[k] e^{j2\pi \frac{kn}{Nfft}}$$

for $0 \le n \le Nfft - 1$ and sub-carriers $0 \le k \le Nfft - 1$. The received signal with channel impulse response hm[n] and AWGN zm[n] is

$$r[n] = \sum_{k=0}^{N_c-1} x_m[k] h_m[n-k] + z_m[n]$$

for channel impulse length Nc. The demodulated symbol is then

$$\overline{X}_m[l] = \sqrt{1Nfft} \sum_{n=0}^{Nfft} \left(r_m[n] \right) e^{-j2\pi \frac{ln}{Nfft}}$$

$$= \sqrt{1Nfft} \sum_{n=0}^{Nfft} \left(\sum_{k=0}^{N_c-1} x_m[k] * h_m[n-k] \right) e^{-j2\pi \frac{ln}{Nfft}}$$

$$= X_m[l] H_m[l] + Z_m[l]$$

where Zm[l] is the FFT of the additive Gaussian noise. Let the correct frame start time be $\zeta = 0$. We assume without loss of generality that $\zeta > 0$ so that the frame includes both the mth and the (m + 1)th OFDM symbol. The selected samples for the FFT window are ym = rm[1], rm[2], · · · , rm[Nfft − 1] and with the frame timing offset the selected samples are ym = rm[ζ], rm[ζ +1], · · · , rm[Nfft −1], rm+1[1], rm+1[2], · · · , rm+1[Nfft −1+ζ]. After a similar derivation, as that presented in section 5.1.2, the demodulated lth symbol of the mth frame is

$$\overline{X}_m[l] = \frac{Nfft-\zeta}{Nfft} X_m[l] H_m[l] e^{j2\pi \frac{\zeta}{Nfft}} + \frac{1}{Nfft} \sum_{k=0}^{Nfft-\zeta-1} X_m[k] H_m[k] \sum_{n=0}^{Nfft-\zeta-1} e^{j2\pi \frac{k-l}{Nfft}n} + \frac{1}{Nfft} \sum_{k=Nfft-\zeta}^{Nfft-1} X_{m+1}[k] H_{m+1}[k] \sum_{n=Nfft-\zeta}^{Nfft-1} e^{j2\pi \frac{k-l}{Nfft}n}$$

The first term is the desired demodulated sub-carrier, but with an attenuation factor as well as a phase rotation. The second term is the ICI component and the third the ISI.

The previous figures show that as the number of sub-carriers increases the effect of the frame timing offset on the attenuation factor decreases. This is explained by the term (Nfft − ζ)/Nfft in equation 6.21.

Consider the frame start positions as presented in Figure 6.2 where there is the addition of a cyclic prefix. There are two possible cases for frame start regions. If the start point is within region A, it is unaffected by the multipath channel and the FFT window is within the correct OFDM symbol. The addition of the cyclic prefix extends the OFDM symbol allowing for the offset FFT window to remain within the correct OFDM symbol. If the start position is within region B, it will either be affected by the multiple paths (an early start) or extend into the next OFDM symbol causing ISI and ICI. Notice that as Nfft increases, the contribution of ICI and ISI decreases as expected from the term 1/Nfft in equation 6.21.

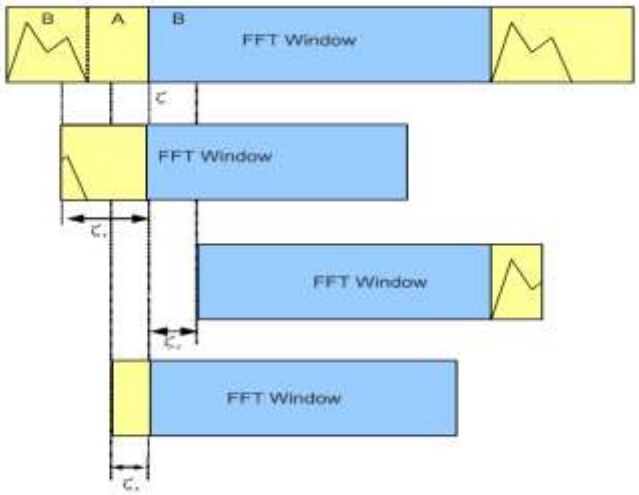

As before (section 5.1.2) the power in the ICI, ISI, and the combination of the two can be found by taking the expected value.

$$ICI_{power} = E\left[ICI_\zeta(l) \overline{ICI_\zeta(l)} \right]$$

$$= E\left[\left(\frac{1}{Nfft} \sum_{k=0}^{Nfft-\zeta-1} X_m[k] H_m[k] \sum_{n=0}^{Nfft-\zeta-1} e^{j2\pi \frac{k-l}{Nfft}n} \right) \times \overline{\left(\frac{1}{Nfft} \sum_{k=0}^{Nfft-\zeta-1} X_m[k] H_m[k] \sum_{n=0}^{Nfft-\zeta-1} e^{j2\pi \frac{k-l}{Nfft}n} \right)} \right]$$

(6.23)

$$= \sigma_x^2 \frac{(Nfft-\zeta)\zeta}{Nfft}$$

$$ISI_{power} = E\left[ISI_\zeta(l) \overline{ISI_\zeta(l)} \right]$$

$$= E\left[\left(\frac{1}{Nfft} \sum_{k=Nfft-\zeta}^{Nfft-1} X_{m+1}[k] H_{m+1}[k] \sum_{n=Nfft-\zeta}^{Nfft-1} e^{j2\pi \frac{k-l}{Nfft}n} \right) \times \overline{\left(\frac{1}{Nfft} \sum_{k=Nfft-\zeta}^{Nfft-1} X_{m+1}[k] H_{m+1}[k] \sum_{n=Nfft-\zeta}^{Nfft-1} e^{j2\pi \frac{k-l}{Nfft}n} \right)} \right]$$

(6.26)

$$= \frac{\sigma_x^2 \zeta}{Nfft}$$

$$Total\ Interference\ Power = E\left[\left(ICI_\zeta(l)+ISI_\zeta(l)\right)\left(ICI_\zeta(l)+ISI_\zeta(l)\right)\right]$$

$$= \frac{\sigma_x^2 (2Nfft-\zeta)\zeta}{Nfft}$$

whereas before $\sigma^2 x$ is the expected power of the received sub-carrier symbols.

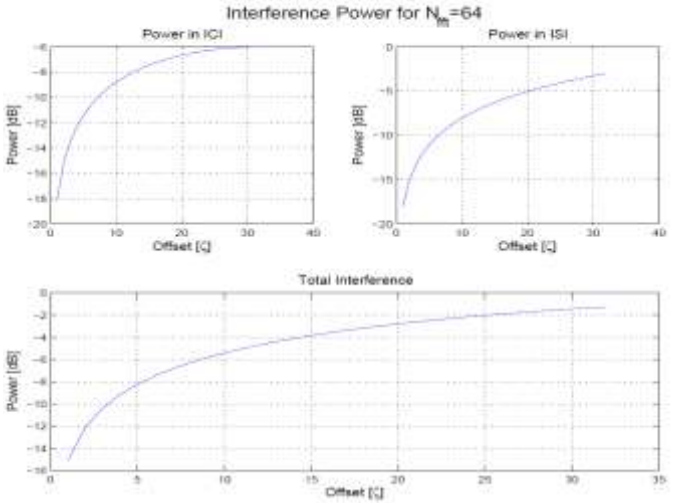

Figure 6.3 Power of ICI, ISI, and total interference for Nfft = 64**.**

Synchronization error estimation: Synchronization is separated into two categories, acquisition and tracking. In acquisition we focus on carrier frequency offset estimation, symbol timing and frame start position using the preamble structure outlined in IEEE802.11a [12]. Tracking occurs after the preamble has been sent and relies on information embedded into each OFDM frame to ensure carrier frequency and sample clock are locked during transmission.

Preamble Structure of IEEE802.11a: Because of the sensitivity that OFDM has to frequency and timing offsets, measurements must be taken to estimate and correct these offsets at the receiver. To accomplish this and other signal processing functions, four OFDM symbols are prepended to the OFDM burst transmission to aid in acquisition. After this preamble is processed, each successive frame contains four pilot symbols that are used for tracking frequency and timing. Both the symbols in the preamble and the pilot symbols are known to the receiver. The first two OFDM frames contain ten short preambles and are used for automatic gain control, diversity selection, timing acquisition, and coarse frequency acquisition. We will focus our attention on the acquisition of timing and frequency. The zero packing has the effect of decreasing the symbol time by four, or Nfft/4, thus yielding the four copies in the time series. Thus, the short training symbols have 2.5 × Nfft symbols. In our application of OFDM, IEEE 802.11a/g, the bandwidth is 20MHz and the sample time is 1/20MHZ = 0.05μs. If we set Nfft = 64, as in IEEE802.11a, there are 16 samples in the short training symbol and so the symbol time is 16 × 0.05μs = 0.8μs. There are ten short training symbols which gives a total time of 8μs.

The short training symbols are generated by taking the IFFT of the following sequence for frequency bins −26 to 26:

$$S_{-26,26} = \sqrt{\frac{13}{6}} *$$

[0, 0, 1 + 1j, 0, 0, 0,−1 −1j, 0, 0, 0, 1 + 1j, 0, 0, 0,−1 −1j, 0, 0, 0, −1 −1j, 0, 0, 0, 1 + 1j, 0, 0, 0, 0, 0, 0, 0,−1 −1j, 0, 0, 0,−1 −1j, 0, 0, 0, 1 + 1j, 0, 0, 0, 1 + 1j, 0, 0, 0, 1 + 1j, 0, 0, 0, 1 + 1j, 0, 0,]

The last two frames of the preamble contain the long training symbols which are used for channel estimation and fine frequency acquisition. The long training symbols are generated by taking the IFFT of the sequence

$L_{-26,26}$ = [1, 1,−1,−1, 1, 1,−1, 1,−1, 1, 1, 1, 1, 1, 1,−1,−1, 1, 1,−1, 1,−1, 1, 1, 1, 1, 0, 1,−1,−1, 1, 1,−1, 1,−1, 1,−1,−1,−1,−1,−1, 1, 1,−1,−1, 1,−1, 1,−1, 1, 1, 1, 1].

The lack of copies in the OFDM frames is from the lack of zero packing in equation 6.31 and so the symbols have length Nfft and, along with the added cyclic prefix, the total length of the long training symbols is 2.5 × Nfft. Again, we set Nfft = 64 so that the long training symbol is 64 samples long. With a sample time of 1/20MHZ = 0.05μs the long training symbol time is 64 × 0.05μs = 3.2μs. There are two long training symbols and a cyclic prefix of length 32 so the total time for the long training symbols is 2 × 3.2μs + 32 × 0.05μs = 8μs.

OFDM Frame Timing Estimation: Timing estimation is broken into two parts, frame timing or packet detection and symbol timing. In both cases

we use the preamble for detection. Here we start with frame timing and exploit the periodicity of the short training symbols using the auto-correlation as described in [23]. From Appendix F, the cross-correlation function is defined as

$$f * g = \sum_{m=-\infty}^{\infty} \overline{f}[-m]\, g[m]$$

The correlation of the signal with a delayed copy of itself is defined as

$$A[n] = \sum_{k=0}^{N} r(k+n)\, \overline{r}[k+n+L]$$

where A[n] is the output, r[n] is the received sequence, L is the length of one short symbol and the length of the delay. There are several algorithms for coarse timing but all use the correlation properties of the short training symbols. In this analysis, the delay and correlate algorithm presented in [23] and [9] is used. Figure 6.24 shows the block diagram for this algorithm.

The top path, P(d), contains the cross-correlator and the bottom path, R(d), contains the auto-correlator. The δ value in the bottom path is to avoid division by zero. The auto-correlator computes the power in the samples and is used to normalize the decision at the threshold detector. The cross-correlator takes advantage of the periodicity in the short training

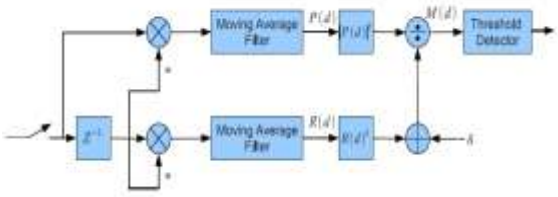

Figure: Delay and correlate algorithm.

symbols to locate the frame boundaries. These are defined mathematically as

$$P(d) = \sum_{m=0}^{L-1} r(d+m)\overline{r(d+m+L)}$$

$$R(d) = \sum_{m=0}^{L-1} \left| r(d+m+L) \right|^2$$

where L is the length of the register in the moving average and r(d) is the dth sample of the received signal. M(d) is the output of the correlator normalized by the received power and then tested against a threshold level. Squaring helps mitigate the effects of large peak to average power ratios common in OFDM. The signal starts after the first 50 samples and because a length of 16 was used for the moving average filter, the maximum value of the correlation and the power is not reached for 16 samples. Also note that the timing estimate M(d) reaches a maximum at the 51st sample, which is the correct timing. One might wonder why the auto-correlation is used in determining the frame start since the cross-correlation shows the symbol boundaries. The received signal will have a carrier frequency offset as well as multipath interference and Gaussian noise. For this reason the auto-correlation function is used to normalize the input to the threshold detector. Even with poor channel conditions the frame is still detected, although with a sample error. This sample error will need to be corrected with fine timing, or symbol timing estimation.

Frequency Offset Estimation: Estimation of frequency offset during the acquisition phase is performed in two parts. Coarse frequency offset uses the short training symbols and fine frequency offset uses the long training symbols. Both coarse and fine frequency estimation use the same algorithm, correlation with the received signal and a delayed copy. The conjugate product is then passed to a phase detector that outputs the phase error. The maximum frequency offset allowed in the IEEE 802.11a standard (section 17.3.9.4) [12] is ±20ppm for carrier frequencies between 5.15 − 5.825GHz. This means that the maximum frequency offset between transmitter and receiver (for carrier frequency 5.825GHz) is

$$f\Delta = \left(40\times10^{-6}\right)\left(5.825\times10^{9}\right)$$
$$= 233KHz$$

Hence any algorithm used to estimate and correct frequency offset needs to operate with this amount of offset. Suppose the received signal is

$$y(t) = x(t)\, e^{j2\pi f \Delta t}$$

where x(t) is the transmitted signal and _f is the frequency offset. As stated previously, the short training symbols have a length of 16 samples or 0.8μs. Then the output of the conjugate product from the correlation of the signal and the delayed copy is

$$y(t)\, y^{*}(t-\delta t) = \left|x(t)\right|^2 e^{j2\pi\Delta f(\delta t)}$$

The frequency offset is found by taking the arctangent of both sides

$$\angle y(t)\,y^*(t-\delta t) = \angle\left|x(t)\right|^2 e^{j2\pi\Delta f(\delta t)}$$

$$\angle y(t)\,y^*(t-\delta t) = 2\pi\Delta f\,\delta t$$

$$\Delta f = \frac{\angle y(t)\,y^*(t-\delta t)}{2\pi ft}$$

where δt is the symbol time. The output of the phase detector is based on the arctangent function and thus has a range of [−π, π). This means that the maximum detectable frequency offset using the conjugate product is

$$\Delta f = \frac{\pm\pi}{2\pi(16)\left(\frac{1}{20GHZ}\right)}$$

$$= \frac{\pm\pi}{2\pi(0.8\mu s)}$$

$$= 625KHZ$$

or about 107ppm at 5.825GHz, much greater than the allowable frequency offset. By comparison, using the long training symbols, the detectable frequency offset is

$$\Delta f = \frac{\pm\pi}{2\pi(64)\left(\frac{1}{20GHZ}\right)}$$

$$= \frac{\pm\pi}{2\pi(3.2\mu s)}$$

$$= 156KHZ$$

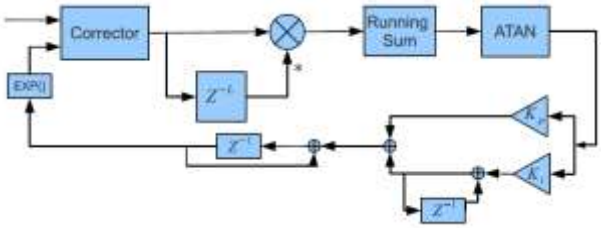

Figure: Frequency estimation algorithm.

This is why the short training symbols are used for the coarse estimation and correction before using the long training symbols for fine frequency estimation and correction. Consider the example where the frequency offset is 200kHzThe poor phase estimation in the long training symbol portion is because the algorithm uses a delay length of 16 where the long training symbols have a length of 64. The previous example did not incorporate a phase locked loop (PLL) but instead the phase estimation of the entire preamble was computed and the average of the phase error was applied to the entire series. This is an impractical implementation because of the delay in waiting for the entire preamble to arrive. We now consider an example which uses a PLL with the same 200kHz frequency offset. By trial and error the values θn = 2π/49 and ζ = √2/2 were found making ki = 0.0594 and kp = 0.1638. The accumulated phase of the variable controlled oscillator (VCO) and the VCO output.. Notice that the frequency is correctly estimated but there is a phase offset in the VCO output. This is referred to as residual frequency offset and is dealt with using the pilot symbols. Lastly, the constellation of the received signal with and without frequency offset compensation. The phase offset seen in the VCO output is also seen in the corrected constellation.

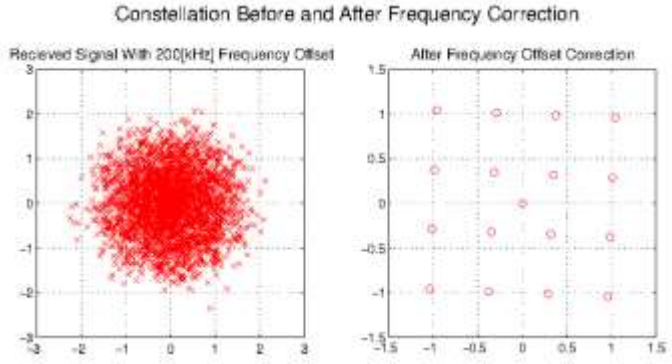

Figure : Constellation with and without frequency offset correction**.**

Symbol Timing Estimation: Symbol timing or fine timing is performed after coarse timing and after frequency offset correction. Fine timing estimation uses the cross-correlation of the known long training symbol with the received long training symbol to determine the start and end of an OFDM symbol and consequently the start and end of the FFT window. As discussed in section 5.2.2, the cross correlation is sensitive to frequency offset and this explains the importance of correcting frequency offset before performing symbol timing estimation. During the frame timing estimation, the starting edge of the packet was determined but within the packet symbol timing errors can be present. The cross-correlation of the known long training symbol and the received long training symbol can be determined by

$$r(n) = \sum_{m=0}^{M} r'_{LTS}(m)\, r_{LTS}(m-n)$$

where r′LTS is the received long training symbols, rLTS is the known long training symbol, and M is the length of the long training symbol. In Appendix F, it is shown that there is a relationship between the cross-correlation operator and the convolution operator. It is desirable to use the convolution operation since it can be performed using the FFT, which reduces the number of computations [19]. Hence, we have the symbol timing estimation as

$$r(n) = r'_{LTS}(n) * r_{LTS}(-n)$$

where $*$ is the convolution operator. There are two and a half long training symbols (the half symbol provided by the cyclic prefix) in the IEEE802.11a standard. Thus the cross-correlation should have three peaks, the first being about half the magnitude of the other two. The first peak corresponds to the end of the cyclic prefix and the other two peaks correspond to the ends of the two long training symbols which have the same length as the OFDM symbol.

Channel Estimation: Let Y be the received signal, X the transmitted signal, and H the channel frequency response. Then

$$Y[k] = H[k]X[k] + Z[k]$$

where Z is the noise. Here we take advantage of the property of Fourier transforms, that convolution in the time domain corresponds to the product in the frequency domain. As stated in Chapter 2, it is assumed that the channel is stationary during each transmitted packet. We have then, setting Z[k] = 0,

$$H[k] = \frac{Y[k]}{X[k]}$$

In this way, the channel can be estimated but only if the transmitted signal is known. To this end, the long training symbols are used. Recall that the long training symbols use all sub-carriers (except DC) so that all used sub-carrier equalizer gains are found. Equation 6.52 describes the channel frequency response for each sub-carrier but the inverse is needed to counter its effects:

Residual Frequency Offset: In Section 6.1.1, carrier frequency offset was simulated and in Section 6.2.3, a method of estimation and correction was put forward. The simulation showed very precise estimation that left the system with negligible errors. In real implementations of frequency offset estimation, the frequency offset is not constant (as simulated in section 6.1.1) and the system itself introduces thermal noise and phase degradation, which increases the error in carrier frequency offset. This error is a residual frequency offset and while it may be small the accumulation of the offset can destroy the orthogonality of the sub-carriers. To continue tracking the frequency offset, each OFDM symbol contains four pilot subcarriers at frequency bins -21, –7, 7, 21 and are BPSK modulated using a pseudo-binary sequence. The scrambler is initiated with all ones and produces the cyclically extended 127 element sequence P0 in equation 6.55:

$P_{0\ldots126v}$={1, 1, 1, 1,−1,−1,−1, 1,−1,−1,−1,−1, 1, 1,−1, 1,−1,−1, 1, 1,−1, 1, 1, −1, 1, 1, 1, 1, 1, 1,−1, 1, 1, 1,−1, 1, 1,−1,−1, 1, 1, 1,−1, 1,−1,−1,−1, 1, −1, 1,−1,−1, 1,−1,−1, 1, 1, 1, 1, 1,−1,−1, 1, 1,−1,−1, 1,−1, 1,−1, 1, 1, −1,−1,−1, 1, 1,−1,−1,−1,−1, 1,−1,−1, 1,−1, 1, 1, 1, 1,−1, 1,−1, 1, −1, 1,−1,−1,−1,−1,−1, 1,−1, 1, 1,−1, 1,−1, 1, 1, 1,−1,−1, 1,−1,−1, −1, 1, 1, 1, 1, 1,−1,−1,−1,−1,−1,−1,−1}

The algorithm for tracking frequency is similar to that of course frequency estimation. After baseband demodulation, the pilots are extracted and the phases of the pilots are compared to the phases of the previous pilots. The phase offset is sent to a loop filter, then to a VCO, and multiplied to the input of the FFT. Appendix G further discusses the phase lock loop and Appendix H contains MATLAB code to simulate the PLL.

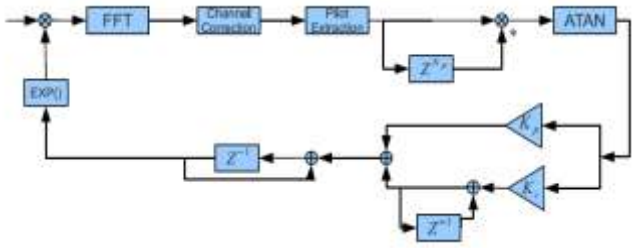

Figure: Residual frequency tracking

THE RESULTS: The following results are observed at the outcome.

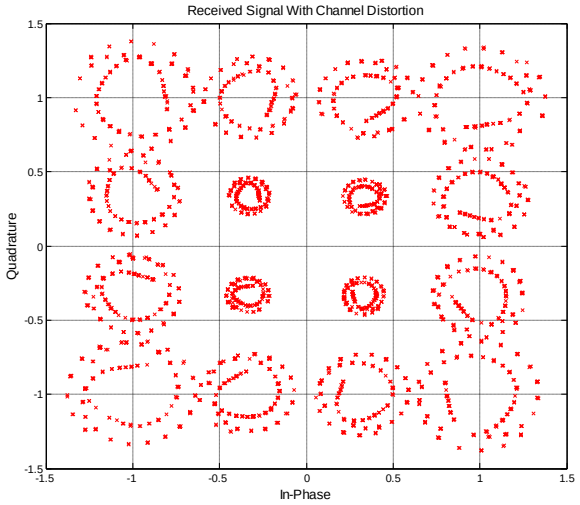

Effects of multipath channel on received constellation.

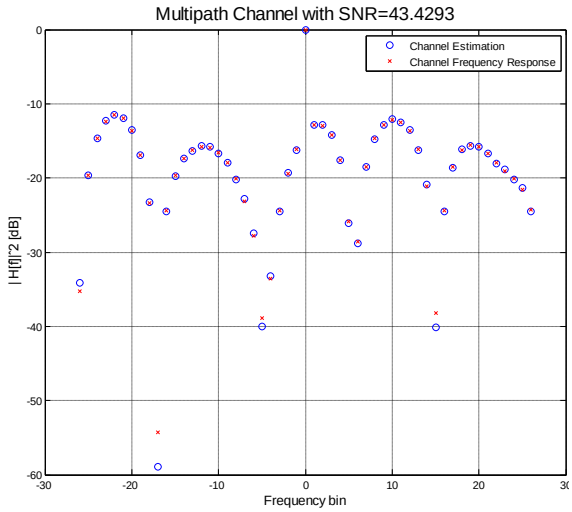

Channel estimation

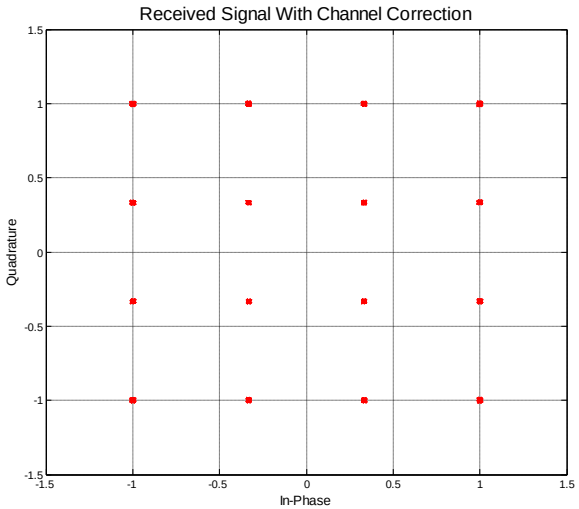

Received constellation after channel correction

CONCLUSION: Following are the areas of future study which should be considered for further research work. Implementation of other interpolation techniques for channel estimation. In this work we have considered only two type interpolation techniques. We can extend this work for other interpolation techniques such as second order, low-pass etc. Feasibility study of Multiple Input Multiple Output (MIMO) OFDM systems. In this study we have discussed about Single Input Single Output (SISO) OFDM systems MIMO OFDM can be implemented using multiple transmitting and receiving antennas which are an interesting work of future.

REFERENCES:

[1] Jan-Jaap van de Beek , Magnus Sandell , Per Ola BÄorjesson ,On Synchronization in OFDM Systems Using the Cyclic Prefix, IEEE 2006

[2]Hindawi Publishing Corporation EURASIP Journal on Wireless Communications and Networking, C.Williams, S. McLaughlin, and M. A. Beach , Robust OFDM Timing Synchronization in Multipath Channels , 21 April 2008

[3]International Journal on Information Theory (IJIT), Vol.3, No.2, April 2014 DOI: 10.5121/ijit.2014.3201 1, Study of Timing Synchronization in MIMO-OFDM Systems Using DVB-T , Farhan Farhan, Electrical Systems Technology Instructor, A-B Tech, Asheville NC, USA

[4]Journal of Signal and Information Processing, 2013, 4, 138-143 doi:10.4236/jsip.2013.43B024, Published Online August 2013, Frequency Synchronization in OFDM System, C. Geetha Priya, A. M. Vasumathi

[5]Sun et al. EURASIP Journal on Wireless Communications and Networking 2012, 2012:368